Anodic Silicon Dissolution in Acidic Fluoride Electrolyte. A Probe Beam Deflection Investigation

Sandro Cattarin,*,† Franco Decker,‡ and Danilo Dini‡

IPELP−C.N.R., Corso Stati Uniti 4, 35100 Padova, Italy, and Dipartimento di Chimica, Università "La Sapienza", 00185 Roma, Italy

Received: January 27, 1998

Si anodic dissolution in acidic fluoride medium has been investigated in different regimes (porous silicon formation, electropolishing under stationary and oscillating current) by probe beam deflection (PBD) or the "mirage" technique. Evolution of deflection signal allows monitoring of dissolution processes both under polarization and at open circuit, providing for example an estimate of the oxide etch-back times during open circuit corrosion. The time evolution of deflection signal during current oscillations reveals components resulting from electrochemical film formation and chemical dissolution. The PBD technique shows larger etching rates for the less passivating film (low potential) and smaller etching rates for the better passivating film (high potential). Our observations are compared with those obtained from spectroscopic investigations of the oxide layer and their relevance for models of oxide formation, and dissolution is here discussed.

1. Introduction

The great technological importance of acidic fluoride media for wet silicon processing (oxide removal, hydrogen passivation, electropolishing, porous silicon formation) has attracted much fundamental and applied research over several decades.[1−6]

Besides electrochemical investigations, the application of in situ and ex situ spectroscopic techniques has provided a firm basis to interpretation of phenomena.[7−12] Hence, it has been shown by in situ infrared study[8,9] that the surface is hydrogen terminated in the region of rising current from open circuit to the first peak (the region of porous silicon formation) and covered by a "wet" oxide and a comparatively more "dry" oxide in the first and second electropolishing plateaus, respectively. A rather linear increase of oxide thickness with applied potential and a slope of 8−10 Å/V have been reported.[9] Several attempts at characterizing oxide formation and dissolution have been performed on the basis of optical techniques able to monitor oxide thickness and quality.[7−12] Evidence has been collected that the oxide generated in the regime of current oscillations has an inhomogeneous depth profile with layers of soft and compact oxide.[12]

The probe beam deflection (PBD) technique is suitable for "in situ" studies of processes in the diffusion layer, e.g., for the monitoring of deposition or dissolution phenomena, since it is contactless, noninvasive, and very sensitive to concentration gradients in the electrolyte.[13−15] Several papers have shown how the study of the mirage effect may provide information on the propagation of concentration waves in an electrolyte as a consequence of oxidation/reduction processes at the electrode.[13−18] In a recent publication[19] the mechanism of an oscillatory reaction at an inert metal electrode has been discussed in light of PBD experiments. The aim of the present paper is to characterize silicon dissolution in acidic fluoride media under the most significant electrochemical conditions by PBD. This seems to be of particular interest for such cases in which the oxide formation/dissolution is not directly controlled by the driving electrochemical variables, i.e., in a regime of sustained potential oscillation and during open circuit dissolution of the oxide formed at a fixed potential.

2. Experimental Section

The (100) oriented silicon wafers (thickness 381 ± 25 μm, resistivity 8−12 Ω cm) were purchased from Semimetrics Ltd., England. The wafers had different surface finishes on the two faces. Silicon crystals about 20 × 8 mm^2 were cut from the wafer and mounted on suitable holders, making the contact with In/Ga eutectic and silver paste. The rough back surface was sealed with a PTFE-coated adhesive tape (Cole Parmer Instruments). Prior to experiments the electrodes were etched for 60 s in a 1:1 mixture of 40% HF:ethanol to remove the oxide layer and rinsed with distilled water. $NH_4F + CH_3COOH$ solutions were prepared from analytical grade commercial products (BDH, Aldrich, or Merck) and triply distilled water, adjusting the pH to 4.5 by addition of NH_3.

The cell used for the probe beam deflection (PBD) measurements was a single-compartment cell with four optical windows and a three-electrode configuration; counter and quasi-reference electrodes were two Pt sheets. All potentials are accordingly given with respect to Pt whose potential in the most frequently used solution (0.2 M NH_4F + 0.1 M CH_3COOH, pH 4.5) was $E = 0.15$ V vs SCE.

The PBD has been measured with a position-sensing photodiode in the photoconductive mode ($V_{bias} = 9$ mV). The photodetector was a model PIN-SPOT 2D from UDT Sensors Inc. (Hawthorne, CA). A He−Ne red laser (=632.8 nm) was used as probe beam. The laser light was focused at the p-Si electrode with a convex lens (focal length = 10 cm). The current output of the position photodetector was converted into the beam deflection angle calibrating the photodetector position with a micrometric screw in the direction normal to the laser light and using the known electrode−photodetector distance.

* Corresponding author.
† IPELP−C.N.R.
‡ Università "La Sapienza".

S1089-5647(98)00896-7 CCC: $15.00
Published on Web 05/19/1998

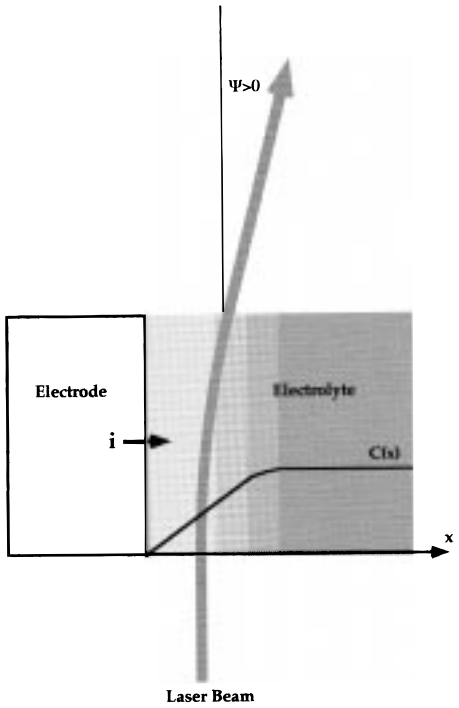

Figure 1. Scheme of probe beam deflection principle. The laser beam deviates toward regions of higher refractive index, namely in most cases toward regions of higher electrolyte concentration.

Beam deflections away from the electrode surface were taken conventionally as positive.[20] Electrochemical measurements were made with a scanning potentiostat EG&G PAR model 362 (Princeton, NJ). Data were acquired and stored in a PC by means of Labview Program from National Instruments Corporation (Austin, TX).

3. Results and Discussion

The laser beam deflection depends on the gradient of electrolyte refractive index in the following way:

$$\psi(x,t) = \frac{l}{n}\left[\left(\sum_i \frac{\partial n}{\partial c_i}\frac{\partial c_i}{\partial x}\right) + \frac{\partial n}{\partial T}\frac{\partial T}{\partial x}\right] \qquad (1)$$

where ψ is the time-dependent deflection angle, x a coordinate perpendicular to electrode surface, l the interaction length (electrode width), n the refractive index of the medium, T the temperature of the solution, and i the index referred to every species in the electrolyte. Equation 1 takes into account the fact that the beam deflection can be calculated by summing that due to each component of the electrolyte separately.[21] The gradients of concentration $\partial c_i/\partial x$ and temperature $\partial T/\partial x$ are taken perpendicular to the electrode surface.[16] In ordinary conditions the thermal effects are negligible, and the relevant term is that associated with the concentration gradients (first term in eq 1). If $\partial n/\partial c_i$ are positive, ψ has the same sign of $\partial c_i/\partial x$ and $\psi > 0$ will correspond to a deflection away from the electrode surface (Figure 1).

3.1. Voltammetric Investigations. Typical results of potential sweep experiments from open circuit to 5 V are reported in Figure 2. It may be noticed that the deflection/potential profile follows basically the current curve and reproduces the oscillations beyond the second current maximum.

In the potential range of porous Si formation, dissolution is a two-electron reaction where the products react with the solvent, forming the species SiF_6^{2-} and hydrogen gas (see eqs 2a and 2b).[3−6] The observed positive deflection is due to a positive gradient of the electrolyte refractive index, as expected when the dominant process is HF consumption (see discussion below). Assuming that the reaction at p-Si proceeds by hole capture (neglecting electron injection that may also occur in this case[22]):

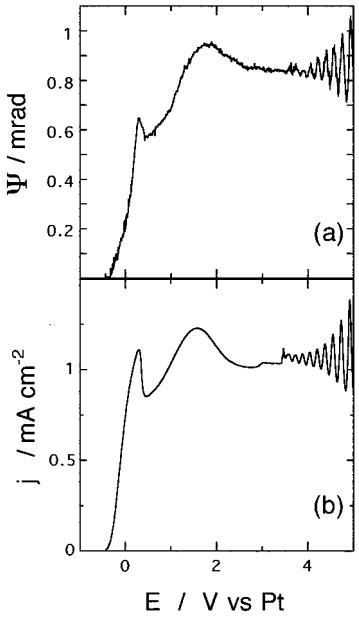

Figure 2. Deflectometric signal (a) recorded during a quasi-stationary current/voltage curve of silicon dissolution (b). Electrolyte: NH_4F 0.2 M, CH_3COOH 0.1 M, pH adjusted to 4.5 with NH_3. Scan rate 10 mV s^{-1}.

$$Si + 2HF + 2h^+ \rightarrow SiF_2 + 2H^+ \qquad (2a)$$

$$SiF_2 + 4HF \rightarrow SiF_6^{2-} + 2H^+ + H_2 \qquad (2b)$$

for an overall stoichiometry

$$Si + 6HF + 2h^+ \rightarrow SiF_6^{2-} + 4H^+ + H_2 \qquad (2)$$

The interface acts, therefore, as a sink of HF and as a source of SiF_6^{2-} and H^+ ions and H_2 molecules. The production of H^+ and SiF_6^{2-} would contribute with a negative deflection, whereas the generation of H_2 should bring about a positive deflection because $\partial n/\partial c_i < 0$ for a dissolved gaseous species.[23] Since the above reaction products have counterbalancing effects on the electrolyte refractive index, we can assume that the consumption of HF with a high stoichiometric factor (reaction 2) is the main responsible for the positive deflection signal in the porous Si potential region.

At higher potentials electropolishing occurs via electrochemical formation of a surface (hydr)oxide and its dissolution by a chemical etching process, the final species being again SiF_6^{2-}:

$$Si + 2H_2O + 4h^+ \rightarrow SiO_2 + 4H^+ \qquad (3a)$$

$$SiO_2 + 6HF \rightarrow SiF_6^{2-} + 2H^+ + 2H_2O \qquad (3b)$$

for the overall stoichiometry

$$Si + 6HF + 4h^+ \rightarrow SiF_6^{2-} + 6H^+ \qquad (3)$$

with a dissolution valence of 4.

From the above considerations the deflection signal ψ in the electropolishing regime, reaction 3, can still be ascribed to HF

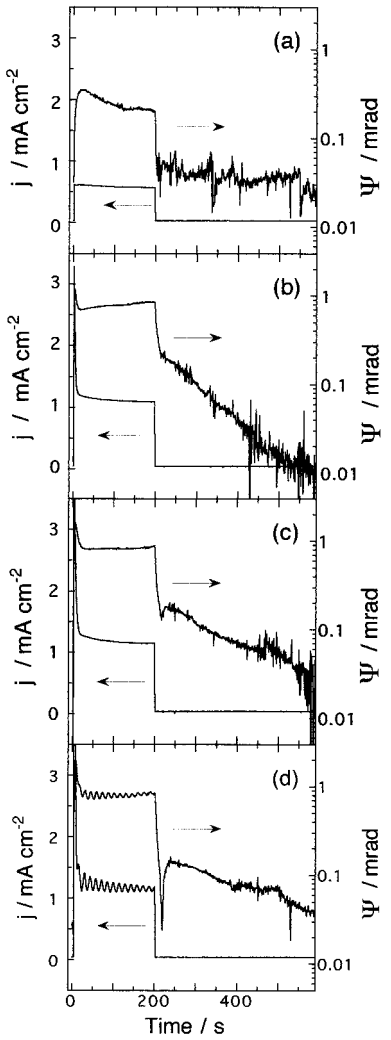

Figure 3. Evolution of current and deflection during potential step experiments from open circuit to (a) 0.0, (b) 1.0, (c) 2.5, and (d) 3.5 V. At $t = 200$ s the cell was disconnected and the electrode was left at open circuit. Same electrolyte as in Figure 2.

consumption but should be less positive than the deflection in reaction 2 because of the absence of H_2 among the reaction products and of the higher number of charges consumed in (3). The experimental observations, on the contrary, have shown larger deflections at higher potentials, for about the same anodic current density (Figure 2). Although there is no apparent reason for this, a possible explanation may be that the Si(II) species is stable enough to diffuse away from the electrode surface. Hence, the chemical process in eq 2b would influence little the signal ψ, which in the region of porous Si formation would mainly depend on the electrochemical process in eq 2a. This would be consistent with the limited formation of gas bubbles on the electrode surface and with the observed values of deflection in the two regions of porous silicon formation and electropolishing: the ratio ψ(electropolishing)/ψ(porous Si) for an equal current is about 1.3, close to the ratio of consumed HF moles per 1 faraday (1.5/1) considering eqs 3b and 2a for the analysis of deflection signal.

3.2. Potential Step Experiments. In a series of experiments (Figure 3) the potential was stepped from open circuit voltage to some values selected on the basis of the quasi-stationary current/voltage curve of Figure 2. The potential was fixed in regions corresponding to different surface conditions: (a) hydrogenated, $E = 0$ V; (b) covered by a "wet" oxide, $E = 1$ V; (c, d) covered by a "dry" oxide, $E = 2.5$ V and $E = 3.5$ V, respectively. After reaching a (rather) steady current, the circuit was open and the relaxation of the deflection signal was recorded.

After cell disconnection the curve shown in Figure 3a shows a drop of deflection to essentially the value of the unperturbed solution over a time of a few seconds. A time in the order of 2−5 s is calculated with a handy rule of thumb for the buildup (and relaxation) of a diffusion layer thickness δ of about 100 μm $= 10^{-2}$ cm in aqueous solution ($\delta = (2Dt)^{1/2}$,[24] $D = (1-3) \times 10^{-5}$ cm^2/s [25]). Hence, the drop of deflection occurs over the time necessary for diffusion phenomena to remove the concentration gradient at the location of the laser beam. Since the curve in Figure 3a is relevant to a potential step in the region of hydrogen termination, no oxide is formed and no dissolution can be observed after cell disconnection. A residual minor decay of ψ may be associated with slow etching of Si from a porous structure[6] whose roughness gradually decreases with etching.

In the experiment of Figure 3b, the potential was stepped in the region between the two peaks, where the surface should be covered by a "wet" oxide. In this case after cell disconnection, we observe first a fairly rapid decay of ψ, which may be discussed as in the previous paragraph, followed by a slower decay which may be reasonably associated with dissolution of a surface (hydr)oxide layer. It is interesting to note that this second decay is monotonic and follows fairly well a negative exponential law: the rate of dissolution decreases steadily with time.

In the experiments of Figure 3c,d the potential was stepped in regions positive with respect to the second peak, where the surface should be covered by a "dry" oxide. By contrast with the previous experiment, when the circuit is open and the current flow interrupted, the deflection signal drops to a minimum, deeper for higher polarization potentials, then recovers to an intermediate value, and subsequently decreases, again with a law close to a negative exponential decay. The deep minimum, not observed in curve b, may be tentatively attributed to a delay in the onset of etching. In this potential region the oxide is compact, and etching, quite slow immediately after interruption of polarization, might need a few seconds of "induction", possibly with occurrence of slow phenomena like pore formation, electrolyte creeping, and gradual conversion of a dry and compact into a wet and porous oxide layer.

Considering the time evolution of ψ after current interruption, it is tempting to see in the exponential law of decay, which is observed for example in Figure 3b, a simple kinetic law of the type valid in the homogeneous phase;[26] however, before elaboration of a thorough model it is safer to conclude merely that the rate of dissolution decreases with time, as would be expected for dissolution of a rough, porous film which becomes gradually thinner and, possibly, smoother and more compact as etching proceeds toward the substrate. The deflection signal in Figure 3c,d decays to a negligible value (say e.g. <0.05 mrad) within about 300 s, which may be regarded as the etch-back time. Considering that under polarization at the given voltage the oxide layer should achieve a thickness in the order of 20−30 Å,[9] the etching time after interruption of polarization suggests an average etching rate in the order of 0.1 Å s^{-1}, in substantial agreement with literature values obtained from measurements of oxide thickness.[6,7]

3.3. Current Oscillations at Constant Imposed Potential. The current oscillations are observed if the potential is stepped in the range 3.5−7 V. In these conditions current oscillations are typically damped (Figure 3d). The insertion of a resistance

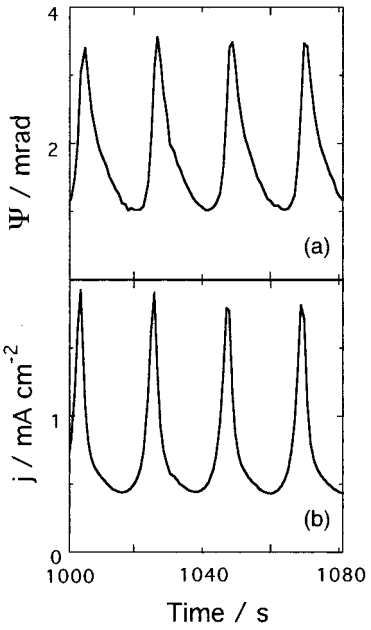

Figure 4. Deflectometric signal (a) recorded in the regime of sustained current oscillations (b) under potentiostatic control ($E = 6$ V vs Pt). A series resistance $R_s = 700\ \Omega$ was inserted in series to the working electrode, with an approximate area of 1 cm^2. Same electrolyte as in Figure 2.

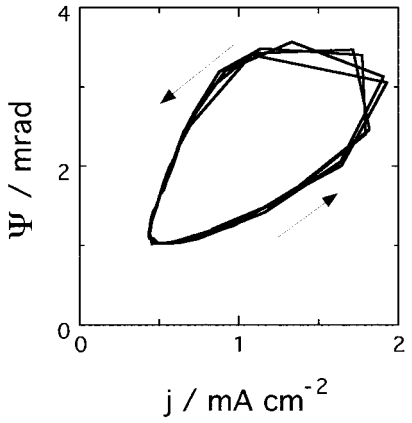

Figure 5. Relation between ψ and current, in the form of Lissajoux plot, for the regime of sustained current oscillations.

in series with the working electrode promotes a regime of sustained oscillations such as in Figure 4, current variations being reflected in similar variations of the deflectometric signal. The shape of the deflection wave (Figure 4a) follows closely the current signal (Figure 4b) when the latter increases and shows a slower relaxation in correspondence to current decrease.

This is better illustrated by the Lissajoux plot reported in Figure 5, in which ψ is reported versus the current density considered as a reference quantity. The relation is not a straight line, as would be expected for two perfectly in-phase parameters, but appears egg-shaped for essentially two reasons: the delay in the ψ response with respect to the current increase, due to diffusion phenomena, and the chemical dissolution rate (eq 3b) which is not constant at the different current values. In fact, once the film has grown thick and blocking, the current drops rapidly and for some time the deflection persists at a larger angle than it was at the corresponding current values for the thin film, due to the larger contribution of chemical dissolution processes.

3.4. Potential Oscillations at Constant Imposed Current. Getting stable galvanostatic oscillations is somewhat difficult. The desired regime of sustained slow oscillations is achieved

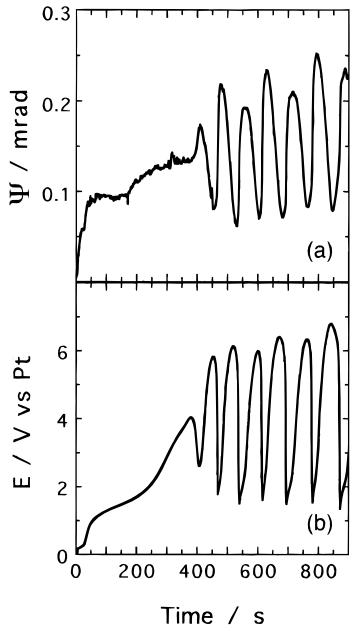

Figure 6. Onset of oscillations for a current step experiment in which a constant current of 250 μA cm^{-2} was imposed at $t = 0$. Time evolution of deflection (a) and potential (b) are shown. Electrolyte: 0.1 M NH_4F, 0.9 M NH_4Cl, 0.1 M CH_3COOH, pH adjusted to 4.5 with NH_3.

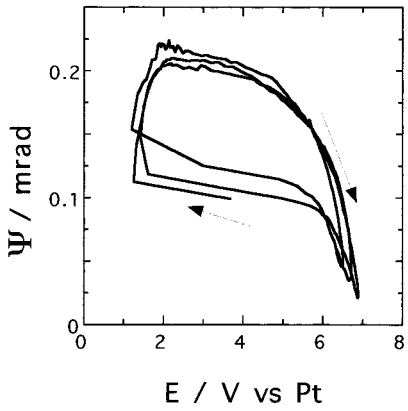

Figure 7. Relation between ψ and potential, in the form of Lissajoux plot, for the regime of sustained potential oscillations.

at pH 4.5 only within a narrow range of imposed current density. In some cases, frequency doubling and transition to a chaotic behavior can be observed. We have obtained regular potential oscillations in the range 0.1−0.2 M NH_4F and pH = 4.5 (acetic buffer).

Figure 6 shows the onset of slow oscillations on imposing a fairly low current density (250 μA cm^{-2}) in 0.1 M NH_4F + 0.9 M NH_4Cl + 0.1 M CH_3COOH, pH 4.5. The potential oscillates between a lower value of about 1.5 V and an upper value around 6 V. The transition from high to low potential is rapid and indicates a sudden collapse of the blocking properties of the film. The backward transition appears comparatively slower, suggesting that the increase of blocking properties occurs gradually by growth of a passivating film. In a first approximation the deflection signal shows a pronounced maximum when the potential is at its minimum and a marked minimum when the potential is maximum.

In Figure 7 we show a Lissajoux figure obtained plotting ψ versus E (reference quantity) in the regime of regular oscillations at longer times with respect to the range shown in Figure 6. This plot emphasizes the correlation between potential and deflection angle ψ and the cyclic nature of phenomena. The

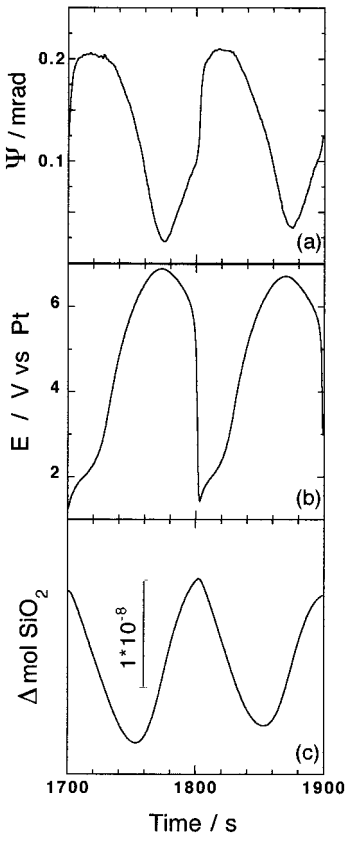

Figure 8. Deflection (a) and potential (b) oscillations under galvanostatic control (same experiment of Figure 6). Part c shows mass variation of surface SiO_2 layer as deduced from the model.

transition of the electrode potential from high to low positive value, indicating a collapse of the passivating surface oxide film, causes with some delay a sudden increase of ψ (see Figure 8a,b). A subsequent increase of the applied potential indicates formation and growth of a better passivating film with a parallel decrease of ψ down to a minimum. In this experiment the current is constant, and the hysteresis observed for example in Figure 7 only reflects variations of chemical processes (eq 3b). Here the delay introduced by diffusion phenomena (a few seconds at most) is much shorter than the period of an oscillation (about 100 s). The same considerations hold for the oscillations of deflection and potential reported respectively in parts a and b of Figure 8, which have been amplified for an easier correlation. In 0.2 M NH_4F, pH 4.5, although the oscillation period is shorter as compared to that in Figure 7, the correlation between curves of potential and deflection is quite similar.[27]

4. Oxide Growth and Dissolution during Galvanostatic Oscillations: A Model

Let us consider the experiments of Figures 6−8, in 0.1 M NH_4F, 0.9 M NH_4Cl, 0.1 M CH_3COOH, pH = 4.5, with a large amount of supporting electrolyte (NH_4Cl) added to the solution. According to eq 1, the deflection angle ψ is proportional to the sum of concentration gradients of the species i in solution at the distance d of the probe beam (coordinate x is perpendicular to electrode surface). If the species i moves only under the effect of diffusion (negligible migration), then the flux $J_i(d,t)$ will be proportional to the concentration gradient as expected from Fick's first law. On this basis, neglecting thermal effects, we can obtain from eq 1 the relationship

$$\psi(d,t) = \sum_i k_i J_i(d,t) \tag{4}$$

k_i being the proportionality constant for the species i in the electrolyte. In the potential oscillation regime the reactions involved are the electrochemical formation of SiO_2 (eq 3a) and its chemical dissolution (eq 3b). Hence, the positive deflection ψ is mainly determined by the HF consumption as previously discussed in section 3.1. Our operating conditions allow simplification of eq 4, since (a) the concentration gradient of the reactants overwhelms that of the products, due to the reaction stoichiometric factors; (b) fast proton diffusion occurs, requiring only small concentration gradients of the latter species;and (c) the role of the supporting electrolyte in the deflection signal can be neglected, because when the refractive index gradients $\partial n/\partial c_i$ for supporting (NH_4Cl) and reactive (NH_4F) electrolytes are quite similar, then ψ depends only on reactive electrolyte flux.[21] An approximate deflection angle ψ can be written as

$$\psi(d,t) \cong \psi_0 + k_{HF}\, J_{HF}(d,t) \tag{5}$$

where ψ_0 is a constant component associated with reaction 3a, and the second term is the variable deflection due to reaction 3b. The constant additive term ψ_0 is presumably small since the fast diffusing hydrogen ions generated during Si oxidation do not contribute with a significant refractive index gradient and because the water solvent is the only other reactant consumed in eq 3a. At the current density $j = 250\ \mu A\ cm^{-2}$ imposed in Figures 6−8, a constant oxide growth rate v_0 of about 6.5×10^{-10} mol cm^{-2} s^{-1} can be calculated (4 e^- process). Since a regime of sustained oscillations is described by closed trajectories in the phase plane (e.g., limit cycles[28]), it is reasonable to think that the interface will look about the same at corresponding potential values separated by entire periods Δt (about 100 s in Figure 8). Hence, about 6.5×10^{-8} mol cm^{-2} of oxide is produced at constant rate v_0 over an entire period and dissolved at variable rate $v_d(t)$ during that period.

The instantaneous net rate of oxide mass change $v(t)$, in mol cm^{-2} s^{-1}, will be $v(t) = v_0 - v_d(t)$. The latter quantity $v_d(t)$ can be estimated by monitoring the HF flux and using eq 5, once the value of k_{HF} is known. The constant k_{HF} may be evaluated by integrating the HF flux in eq 5 (simplified by neglecting ψ_0) over an entire period Δt:

$$\Delta \mathrm{mol}_{HF} = \frac{\int_t^{t+\Delta t} \psi(d,t)\, dt}{k_{HF}} = 6\Delta \mathrm{mol}_{SiO_2} \tag{6}$$

where $\Delta \mathrm{mol}_{SiO_2}$ is the number of SiO_2 moles produced and removed over one complete oscillation per unit electrode area. Equation 6 allows estimating the phenomenological constant k_{HF} since $\Delta \mathrm{mol}_{SiO_2}$ is obtained by application of Faraday's law in eq 3 and $\psi(d,t)$ is a measured quantity. In our experiment $k_{HF} = 3.3 \times 10^4$ rad mol^{-1} cm^2 s.

The variable oxide dissolution rate $v_d(t)$ can be now estimated using simplified eq 5,

$$v_d(t) = (1/6)J_{HF}(d,t) = \{[1/(6k_{HF})]\psi(d,t)\} \quad \mathrm{mol\ cm^{-2}\,s^{-1}} \tag{7}$$

and the net rate of oxide mass change $v(t)$ in mol cm^{-2} s^{-1} will be given by

$$v(t) = v_0 - v_d(t) = \{(6.5 \times 10^{-10}) - (5 \times 10^{-6}\psi(d,t))\} \quad \mathrm{mol\ cm^{-2}\,s^{-1}} \tag{8}$$

where $\psi(d,t)$ is expressed in rad. Negative values of $v(t)$ will correspond to a net consumption of electrochemically grown SiO_2 film, whereas positive values $v(t)$ will be associated with a net growth of the oxide layer. By integration of $v(t)$ over time, we obtain the amount $\Delta mol_{SiO_2}(t)$, whose variation during the potential oscillations of Figure 8b is shown in Figure 8c. The time corresponding to the lower potential value has been chosen as the starting point of the oscillation. Within the approximation that SiO_2 density is constant and the film thickness varies homogeneously over the surface during a potential oscillation, the $\Delta mol_{SiO_2}(t)$ profile shown in Figure 8c allows calculation of thickness variation, if the electrode area is known (1 cm^2 in our experiments). Assuming for SiO_2 a density equal to 2.2 g cm^{-3}, we obtain a value of about 4 nm for the variation of oxide thickness during an oscillation, in substantial agreement with values obtained by other in situ techniques.[10,11]

The time evolution of the oxide thickness depicted in Figure 8c is in good agreement with that presented by Lehmann[10] on the basis of ellipsometric investigations of the surface oxide film. In fact, by monitoring $\psi(d,t)$ we have confirmed a rapid increase of dissolution rate in coincidence with the potential drop and with the sudden increase in roughness and stress shown by Lehmann.[10] Comparison of parts b and c of Figure 8 shows that maximum applied potential is necessary when the oxide layer is close to its minimum thickness and minimum potential when the oxide layer is still close to maximum thickness. This observation strongly suggests the presence of oxidic films of (at least) two different types, one compact and highly passivating and the other porous; the potential drop must be associated with a sudden phase transition.[10,29]

All of these observations may be interpreted in the following mechanistic way: the oxide layer grows during constant current experiments as a compact phase from the substrate and is continuously converted on the solution side by chemical degradation into a soft oxide, little passivating (probably hydrated silica). When the thickness of compact oxide exceeds a certain value, a rapid transition occurs with formation of a phase better able to accommodate stress. This transition leads to a drop of the overvoltage necessary to sustain the imposed current and to the formation of a rippled morphology as detected by atomic force microscopy.[10] The compact oxide is massively converted into soft oxide, more permeable to water and ions, with a great increase in dissolution rate. The resulting net growth rate $v(t)$ becomes negative, causing a gradual decrease of the total oxide thickness. Proceeding in time, the compact oxide grows thicker whereas the soft oxide becomes thinner. As a consequence, even the dissolution rate decreases and finally becomes smaller than the formation rate, so that a positive net growth rate $v(t)$ is recovered. The oxide layer thickness grows again, and the cycle starts anew. The presence of phases with very different blocking ability and dissolution rates seems to play a key role in the onset of the observed oscillating mechanism.

5. Summary and Conclusions

The mirage technique is a useful tool to study the processes of (electro)dissolution of silicon in acidic fluoride media both under polarization and at open circuit.

1. In experiments of current interruption the deflection response allows monitoring the processes of oxide etch-back; the time dependence of the etching rate provides information on the film depth profile, showing for example the presence of layers more or less prone to corrosion, and indicates the end point.

2. In the regime of current oscillations (potentiostatic control) the deflection response follows basically the current signal, namely the rate of film formation, but shows even slower components, associated with film dissolution and more visible during the phase of current decay.

3. In the regime of potential oscillations (galvanostatic control) the variations of deflection response allow monitoring the dissolution rate. The rapid transition of electrode potential from high to low is apparently associated with (and most probably originates from) a structural modification of the compact oxide layer resulting in increased etching rate and dissolution. Observations are consistent with the intuitive concept that the film better passivating is also less prone to corrosion, and vice versa.

4. A model has been proposed for the film thickness variation in the regime of potential oscillations. From our findings it resulted that film thickness varies with the same periodicity of potential, achieving its maximum close to the downward potential transition.

References and Notes

(1) Turner, D. R. *J. Electrochem. Soc.* **1958**, *105*, 402.

(2) Gerischer, H.; Lübke, M. *Ber. Bunsen-Ges. Phys. Chem.* **1988**, *92*, 573.

(3) Zhang, X. G.; Collins, S. D.; Smith, R. L. *J. Electrochem. Soc.* **1989**, *136*, 1561.

(4) Eddowes, M. J. *J. Electroanal. Chem.* **1990**, *280*, 297.

(5) Gerischer, H.; Allongue, P.; Costa Kieling, V. *Ber. Bunsen-Ges. Phys. Chem.* **1993**, *97*, 753.

(6) Searson, P. C. In Gerischer, H., Tobias, C. W., Eds.; *Advances in Electrochemical Science and Engineering*; VCH: Weinheim, Federal Republic of Germany, 1995; Vol. 4.

(7) Lewerenz, H. J. *Electrochim. Acta* **1992**, *37* , 847.

(8) Ozanam, F.; Chazalviel, J.-N. *J. Electron Spectrosc. Relat. Phenom.* **1993**, *64/65*, 395.

(9) Da Fonseca, C.; Ozanam, F.; Chazalviel, J.-N. *Surf. Sci.* **1996**, *365* ,1.

(10) Lehmann, V. *J. Electrochem. Soc.* **1996**, *143*, 1313.

(11) Cattarin, S.; Chazalviel, J.-N.; Da Fonseca, C.; Ozanam, F.; Peter, L.; Schlichthörl, G.; Stumper, J. *J. Electrochem. Soc.* **1998**, *145*, 498.

(12) Chazalviel, J.-N., personal communication.

(13) Boccara, A. C.; Fournier, D.; Badoz, J. *Appl. Phys. Lett.* **1980**, *36*, 180.

(14) Decker, F.; Neunschwander, R. T.; Cesar, C. L.; Penna, A. F. S. *J. Electroanal. Chem.* **1987**, *228*, 481.

(15) Russo, R. E.; McLarnon, F. R.; Spear, J. D.; Cairns, E. J. *J. Electrochem. Soc.* **1987**, *134*, 2783.

(16) Fracastoro-Decker, M.; Decker, F. *J. Electroanal. Chem.* **1989**, *266* , 215.

(17) Plichon, V.; Besbes, S. *J. Electroanal. Chem.* **1990**, *284* , 141.

(18) Rosolen, J. M.; Fracastoro-Decker, M.; Decker, F. *J. Electroanal. Chem.* **1993**, *346*, 119.

(19) Kertesz, V.; Inzelt, G.; Barbero, C.; Kotz, R.; Haas, O. *J. Electroanal. Chem.* **1995**, *392*, 91.

(20) Rosolen, J. M.; Decker, F.; Fracastoro-Decker, M.; Gorenstein, A.; Torresi, R. M.; Cordoba de Torresi, S. I. *J. Electroanal. Chem.* **1993**, *354*, 273.

(21) Rosolen, J. M.; Fracastoro-Decker, M.; Decker, F. *J. Electroanal. Chem.* **1994**, *365*, 165.

(22) Cattarin, S.; Peter, L. M. *J. Phys. Chem. B* **1997**, *101*, 407.

(23) O'Brien, R. N. In *Physical Methods of Chemistry*; Weissberger, A., Rossiter, B. W., Eds.; Wiley-Interscience: New York, 1972; Part 3A, pp 1−73.

(24) Bard, A. J.; Faulkner, L. R. *Electrochemical Methods*; Wiley: New York, 1980.

(25) . *CRC Handbook of Chemistry and Physics*, 69th ed.; Weast, R. C., Ed.; CRC Press: Boca Raton, FL, 1988.

(26) Laidler, K. J. *Chemical Kinetics*; McGraw-Hill: London, 1965.

(27) Dini, D.; Cattarin, S.; Decker, F. *J. Electroanal. Chem.*, in press.

(28) Wojtowicz, J. In *Modern Aspects of Electrochemistry*; J. O'Bockris, M., Conway, B. E., Eds.; Plenum Press: New York, 1972; Vol. 8, pp 47−120.

(29) Lewerenz, H.-J. *J. Phys. Chem. B* **1997**, *101*, 2421.